Molecular Neurobiology (2021) 58:2955–2962
https://doi.org/10.1007/s12035-021-02300-5

Dexpramipexole Enhances K^+ Currents and Inhibits Cell Excitability in the Rat Hippocampus In Vitro

Elisabetta Coppi[1] · Daniela Buonvicino[2] · Giuseppe Ranieri[2] · Federica Cherchi[1] · Martina Venturini[1] · Anna Maria Pugliese[1] · Alberto Chiarugi[2]

Received: 12 October 2020 / Accepted: 15 January 2021 / Published online: 10 February 2021

Abstract

Dexpramipexole (DEX) has been described as the first-in-class F1Fo ATP synthase activator able to boost mitochondrial bioenergetics and provide neuroprotection in experimental models of ischemic brain injury. Although DEX failed in a phase III trial in patients with amyotrophic lateral sclerosis, it showed favorable safety and tolerability profiles. Recently, DEX emerged as a Nav1.8 Na^+ channel and transient outward K^+ (I_A) conductance blocker, revealing therefore an unexpected, pleiotypic pharmacodynamic profile. In this study, we performed electrophysiological experiments in vitro aimed to better characterize the impact of DEX on voltage-dependent currents and synaptic transmission in the hippocampus. By means of patch-clamp recordings on isolated hippocampal neurons, we found that DEX increases outward K^+ currents evoked by a voltage ramp protocol. This effect is prevented by the non-selective voltage-dependent K^+ channel (Kv) blocker TEA and by the selective small-conductance Ca^{2+}-activated K^+ (SK) channel blocker apamin. In keeping with this, extracellular field recordings from rat hippocampal slices also demonstrated that the compound inhibits synaptic transmission and CA1 neuron excitability. Overall, these data further our understanding on the pharmacodynamics of DEX and disclose an additional mechanism that could underlie its neuroprotective properties. Also, they identify DEX as a lead to develop new modulators of K^+ conductances.

Keywords Hippocampal neurons · K^+ channels · Population spike · Synaptic transmission · Neuronal excitability

Introduction

In spite of the remarkable therapeutic achievements obtained in various fields of human pathology, the identification of drugs able to counteract neurodegeneration is still an unmet need. The cause of repetitive failures of the hundreds of clinical trials with compounds targeting different mechanisms involved in neuronal cell death resides, for the most part, in the exquisite vulnerability of neurons and their placement behind the blood brain barrier. In this regard, it is still debated whether the concept of the so-called magic bullet, i.e., a compound with absolute selectivity towards a single molecular target, is still valid in the field of neuroprotection. Indeed, although lack of selectivity increases the chance of translational failure due to side effects, evidence indicates that numerous compounds routinely used in the clinics, such as antiepileptics, exert their therapeutic effects because of more than one mode of action. Hence, it is now appreciated that the requirement for absolute target selectivity may have hindered the identification of clinically relevant neuroprotective agents.

In this scenario, the identification of dexpramipexole (DEX) as a pleiotypic neuroactive agent may represent a remarkable achievement with a realistic translational potential to treatment of CNS disorders. DEX is the dextro enantiomer of the potent dopamine D2/D3 receptor agonist antiparkinson drug pramipexole [18]. However, at variance with its isomer, DEX shows negligible affinity for dopamine receptors, and, indeed, the antiparkinson formulation exclusively contains L-pramipexole. Although unable to bind dopamine receptors, DEX is endowed with neuroprotective properties as demonstrated in numerous in vivo and in vitro experimental settings [6, 7, 23, 26, 27]. In particular, DEX was originally identified as the first-in-class F1Fo-ATP synthase activator able to increase ATP production, reduce O_2 consumption, and support neuronal bioenergetics [1, 2, 25]. Thanks to its targeting of

✉ Elisabetta Coppi
elisabetta.coppi@unifi.it

[1] Department of Neurosciences, Psychology, Drug Research and Child Health (NEUROFARBA), Section of Pharmacology and Toxicology, University of Florence, Florence, Italy

[2] Department of Health Sciences, Section of Clinical Pharmacology and Oncology, University of Florence, Florence, Italy

F1Fo-ATP synthase, and the contribution of the latter to build up the macromolecular complex of the mitochondrial permeability transition pore, DEX prevents Ca^{2+}- or hypoxia-induced mitochondrial swelling, thereby preserving organelle functioning and Ca^{2+} homeostasis in injured neurons [6, 11, 27, 29]. In keeping with this, DEX affords protection in multiple models of in vitro excitotoxicity as well as in vivo cerebral ischemia [6, 27]. Because of its neuroprotective potential, DEX reached advanced phases in clinical development for amyotrophic lateral sclerosis [15–17]. Unfortunately, the drug failed to delay disease progression and extend survival in phase III, showing however a good safety and tolerability profile in hundreds of patients receiving the compounds for almost one year. The drug is now under development as an eosinophil-lowering agent [19].

Besides the impact of DEX on F1Fo-ATP-synthase, recent work identified additional molecular properties of the compound, revealing its complex pharmacodynamic profile. Reportedly, DEX inhibits I_A K^+ currents in rat hippocampal neurons, thereby promoting LTP in the CA1 region [13]. In keeping with these electrophysiological effects, the drug improves learning and memory in rat challenged with multiple memory tasks [13]. Additional work shows that DEX prompts a selective block of mouse Nav1.8 Na^+ channels at submicromolar concentrations. In keeping with the key role of these channels in sustaining action potentials of primary nociceptive neurons, DEX increases pain thresholds and provides analgesia in multiple experimental pain models [30].

Because of the intrinsic translational potential of DEX in neurodegenerative disorders, as well as its pleiotypic pharmacodynamic properties, we planned to further investigate the drug's impact on neuronal excitability. We report here that DEX increases outward K^+ currents and reduces neuronal excitability by targeting TEA-sensitive voltage-activated K^+ (Kv) channels and apamin-sensitive small-conductance Ca^{2+}-activated K^+ (SK) channels.

Materials and Methods

Cell Cultures and Patch-Clamp Recordings

All animal procedures were conducted according to the Italian Guidelines for Animal Care, DL 26/2014, and authorized by the Italian Ministry of Health, Aut. N. 788/2016-PR. Primary hippocampal neurons were prepared from embryonic day 17 Wistar rats (Charles River, Italy) as described [8, 13]. Neurons (1.5×10^5 cells/well) were cultured in Neurobasal™ medium with B-27 supplement (GIBCO) and 0.5 mM glutamine on poly-L-lysine-coated coverslips. Whole-cell patch-clamp recordings were performed starting from 14 DIV (days in vitro) as described [12, 14], in order to allow in vitro maturation of neuronal parameters [4]. Each coverslip was transferred to a recording chamber (1 ml) mounted on the platform of an inverted microscope (Olympus CKX41, Milan, Italy) and superfused at a flow rate of 1.5 ml/min with a standard extracellular solution containing (mM): HEPES 10, D-glucose 10, NaCl 147, KCl 4, $MgCl_2$ 1, and $CaCl_2$ 2 (pH adjusted to 7.4 with NaOH). Borosilicate glass electrodes (Harvard Apparatus, Holliston, MA, USA) were pulled with a Sutter Instruments puller (model P-87) to a final tip resistance of 3–6 MΩ. Pipette solution contained (mM): K-gluconate 130, NaCl 6, $MgCl_2$ 2, $CaCl_2$ 5, Na_2-ATP 2, Na_2-GTP 0.3, EGTA 10, and HEPES 10 (pH adjusted to 7.4 with KOH). When indicated, EGTA concentration was lowered to 5 or 0.1 mM. In some experiments, intra- and extracellular KCl was replaced by equimolar CsCl in order to block K^+ channels.

The calculated liquid junction potential in our experimental conditions was -8.94 mV [5], and this value was not subtracted. Data were acquired with an Axopatch 200B amplifier (Axon Instruments, CA, USA), stored, and analyzed with a pClamp 9.2 software (Axon Instruments, CA, USA). All the experiments were carried out at room temperature (20–22 °C). Cell membrane capacitance (Cm) and access resistance (Rs) were routinely monitored by a ± 10 mV voltage pulse and compensated. Only cells with stable (less than 20% change) Cm and Rs were included in the analysis. Current amplitude (measured as pA) was normalized to respective cell capacitance (Cm, measured in pF) and expressed as current density (pA/pF) in averaged results.

A voltage ramp protocol (800 ms depolarization from + 80 to -120 mV) was recorded every 15 s to evoke overall voltage-dependent currents before, during, and after drug treatments. Control ramps during baseline (bsl) were obtained by averaging the last 4 traces (1 min) before drug application and were compared to those measured between 3 and 5 min of superfusion. Net DEX-activated currents were obtained by subtraction of the control ramp from the ramp recorded in the presence of the compound. All drugs were applied by superfusion with a three-way perfusion valve controller (Harvard Apparatus, Holliston, MA USA) after a stable baseline of ramp-evoked currents was obtained. A complete exchange of bath solution in the recording chamber was achieved within 28 s, and this delay was taken into account in our calculations.

Concentration-response curve of DEX effect on outward K^+ currents was obtained by fit of data to four-parameter logistic equation Y = min + (max - min) / 1 + $10^{(\mathrm{LogEC50\text{-}X)nH}}$, where EC_{50} is the half-maximally effective concentration, X is the logarithm of concentration, n_H is the Hill coefficient, and *min* and *max* are the bottom and the top of the curve, respectively. Data were obtained from 82 cells isolated from 10 rats.

Hippocampal Slices and Extracellular Field Recordings

Preparation of Slices

Slices were prepared as previously described [10, 21]. Animals were killed with a guillotine under anesthesia with isoflurane (Baxter, Rome, Italy), and hippocampi was rapidly removed and placed in ice-cold oxygenated (95% O2–5% CO2) artificial cerebrospinal fluid (aCSF) of the following composition (mM): NaCl 124, KCl 3.33, KH_2PO_4 1.25, $MgSO_4$ 1.4, $CaCl_2$ 2.5, $NaHCO_3$ 25, and D-glucose 10. Slices (400 μM nominal thickness) were cut using a McIlwain Tissue Chopper (Mickle Laboratory Engineering Co. Ltd., Gomshall, UK) and kept in oxygenated aCSF for at least 1 h at room temperature. A single slice was then placed on a nylon mesh, completely submerged in a small chamber (0.8 ml), and superfused with oxygenated aCSF (31–32 °C) at a constant flow rate of 2 ml/min. The treated solutions reached the preparation in 60 s, and this delay was taken into account in our calculations.

Test pulses (80 μs, 0.066 Hz) were delivered through a bipolar nichrome electrode positioned in the *stratum radiatum* of the CA1 region of the hippocampus to stimulate the Schaffer collateral-commissural pathway. Evoked potentials were extracellularly recorded with glass microelectrodes (2–10 MΩ, Harvard Apparatus LTD, United Kingdom) filled with 150 mM NaCl. The recording electrode was placed at the dendritic level of the CA1 region (*stratum radiatum*) to record field excitatory postsynaptic potentials (fEPSPs) or, alternatively, in the somatic cell layer of CA1 pyramidal neurons (*stratum pyramidale*) to record population spikes (PSs) as the result of the synchronous action potential firing of a population of cells. Responses were amplified (× 200, BM 622, Mangoni, Pisa, Italy), digitized (sample rate, 33.33 kHz), and stored for later analysis with LTP (version 2.30D) program [3]. Synaptic transmission was monitored by measuring the initial slope (between 20 and 80% of maximal amplitude) of the fEPSP trace. Postsynaptic pyramidal cell excitability was quantified by measuring the PS amplitude, which reflects the number of neurons firing an AP, or latency, which reflects the latency between dendrite depolarization evoked by synaptic glutamate release and the initiation of AP in the soma-axon hillock. Input-output curves were obtained strength at the beginning of each experiment by gradually increasing the stimulus in order to set the stimulus strength as 40–50% of the maximal response. Baseline values for fEPSP or PS were taken during the last 5 min before drug application. The effect of DEX was quantified between 5 and 10 min (5–10 min) or between 25 and 30 min (25–30 min) of DEX application, as indicated. Data were obtained from 18 slices prepared from 9 male Wistar rats (4–6 weeks old).

Drugs

Dexpramipexole (DEX), tetraethylammonium (TEA), (±)-5-(Aminosulfonyl)-N-[(1-ethyl-2-pyrrolidinyl)methyl]-2-methoxybenzamide (sulpiride), apamin, 4-amynopyridine (4-AP), and ethylene glycol-bis(2-aminoethylether)-*N,N,N′,N′*-tetraacetic acid (EGTA) were obtained from Sigma-Aldrich (http://www.sigmaaldrich.com). All drugs were dissolved in distilled water, stored at -20 °C as 10^3 to 10^4 times more concentrated stock solutions, and dissolved daily in the extracellular solution to the final concentration and applied by bath superfusion with a three-way perfusion valve controller (Harvard Apparatus, Holliston, MA USA) after a stable baseline of ramp-evoked currents was obtained. A complete exchange of bath solution in the recording chamber was achieved within 28 s.

Data Analysis

Data are expressed as mean ± SE. Normality of data was assessed by Shapiro-Wilk normality test. All the data were normally distributed. Student's paired, unpaired 2-tailed *t*-tests, or one-way ANOVA followed by Bonferroni's post hoc analysis were performed, as appropriate, in order to determine statistical significance (set at $p < 0.05$). Data were analyzed using software package GraphPad Prism (GraphPad Software, San Diego, CA, USA).

Results

DEX Activates Outward K^+ Currents in Isolated Rat Hippocampal Neurons

Reportedly, DEX efficiently protects brain and neurons from histological and functional damage due to excitotoxic and ischemic insults by improving mitochondrial bioenergetics [27]. In light of the ability of the compound to also target Nav1.8 [30] and I_A [13], we planned to further investigate its effects on neuronal excitability. To this aim, we performed patch-clamp recordings on primary cultures of rat hippocampal neurons and applied a voltage ramp protocol in order to elicit overall voltage-dependent currents in the absence or presence of DEX.

As shown in Fig. 1a, the compound increased ramp-evoked outward currents in cultured hippocampal neurons. The net DEX-sensitive current, obtained by subtraction of the control ramp from that recorded in DEX, is an outward conductance activated by voltages above -60 mV (Fig. 1b), peaking 2–3 min after application (Fig. 1c). A significant increase (from 242.1 ± 18.8 to 319.5 ± 24.4 pA/pF: 32% increase) in outward ramp-evoked currents was induced by the compound in 15 cells tested (Fig. 1d,e). Of note, when intra- and extracellular

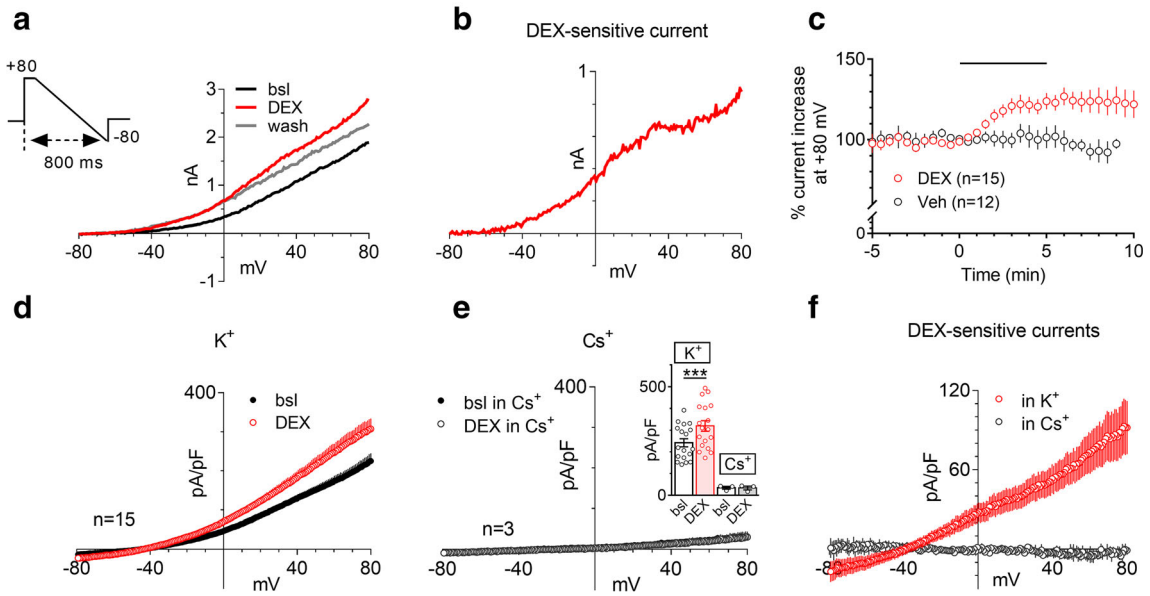

Fig. 1 DEX activates voltage-dependent outward K^+ currents in isolated rat hippocampal neurons. **a** Original patch-clamp current traces recorded in a representative hippocampal neuron where a voltage ramp protocol (+80/-1280 mV, 800 ms: left inset) was applied in control conditions (baseline: bsl), during 10 μM DEX application, or after 5 min wash out. **b** DEX-sensitive current, obtained by subtraction of the control ramp from the trace recorded in DEX, in the same cell. **c** Averaged (mean ± SE) time courses of DEX- (red circles, $n = 15$) or vehicle- (black circles, $n = 12$) mediated effects on ramp-evoked currents at + 80 mV. **d** Averaged ramp-evoked currents measured during bsl or in 10 μM DEX in 15 cells investigated. Inset: % ramp-evoked current increase at + 80 mV before, during, or after the application of DEX (open circles) or its vehicle (Veh, filled circles). **e** Averaged ramp-evoked currents, evoked in bsl conditions or in 10 μM DEX, recorded by using a Cs^+-based pipette solution and a Cs^+-containing extracellular solution. Inset: pooled data of ramp-evoked currents at + 80 mV in standard (K^+-) or Cs^+-based conditions. ***$p < 0.001$, paired Student's t test, $n = 15$. **f** Averaged DEX-sensitive currents recorded in standard (K^+) conditions (in K^+; $n = 15$) or in Cs^+ replacement conditions (in Cs^+; $n = 3$)

K^+ was replaced by equimolar Cs^+, the ramp failed to induce outward currents with DEX loosing its enhancing effect (Fig. 1e,f), thereby indicating an involvement of outward K^+ currents.

As shown in Fig. 2, the effect of DEX was concentration-dependent (Fig. 2a; EC_{50} = 350 ± nM 95% confidence limits: 107.2 nM–1.14 μM: Fig. 2b) and was not affected by reducing the intracellular concentration of EGTA from 10 mM (our control condition) to 5 or 0.1 mM (Fig. 2c). In keeping with the Cs^+ replacement experiments, the effect of DEX was prevented by the unselective K^+ channel blocker TEA (3 mM: Fig. 2d), thereby indicating the involvement of outward voltage-dependent Kv channels. Conversely, neither big-conductance Ca^{2+}-dependent K^+ (BK) channel block by low TEA (0.2 mM) nor I_A inhibition by 4-AP affected DEX-sensitive currents (Fig. 2e,f). Interestingly, however, the latter was reduced by the selective SK channel blocker apamin (Fig. 2e,f).

It is known that DEX is a weak agonist at dopaminergic D2/D3 receptors, the affinity being 10^3–10^4 times lower than that of its enantiomer pramipexole [18]. Thus, to rule out an involvement of dopaminergic receptors in mediating the effects of DEX on outward K^+ currents, we reproduced the experiments in the presence of the prototypical and potent D2/D3 antagonist sulpiride, applied at saturating concentration (1 μM) [20]. Notably, under these conditions, DEX increased outward K^+ current (Fig. 3a–c) to an extent similar to that obtained without sulpiride (Fig. 3d).

DEX Inhibits Synaptic Transmission and Pyramidal Neuron Excitability in CA1 Rat Hippocampal Slices

Next, we wondered whether the ability of DEX to potentiate outward K^+ currents can affect neurotransmission in an integrated system. To this end, we performed extracellular field recordings in acute rat hippocampal slices evaluating fEPSP slope in the CA1 dendrites, as an index of synaptic activity, and PS amplitude and latency in the CA1 pyramidal cell layer, as an index of postsynaptic neuronal excitability. Of note, DEX did not significantly affect the amplitude of the afferent fiber volley (Fig. 4c).

As shown in Fig. 4a, a 30-min application of DEX reduced excitatory synaptic transmission in the CA1 stratum radiatum. The inhibitory effect was transient, with the fEPSP slope returning to basal values within 25–30 min (Fig. 4b). In keeping with fEPSP slope reduction, DEX also decreased amplitude and increased latency of evoked PSs (Fig. 5a,c). The effect of DEX on PS amplitude also declined within 25–30 min (Fig. 5b), whereas the effect on PS latency persisted throughout the application (Fig. 5d).

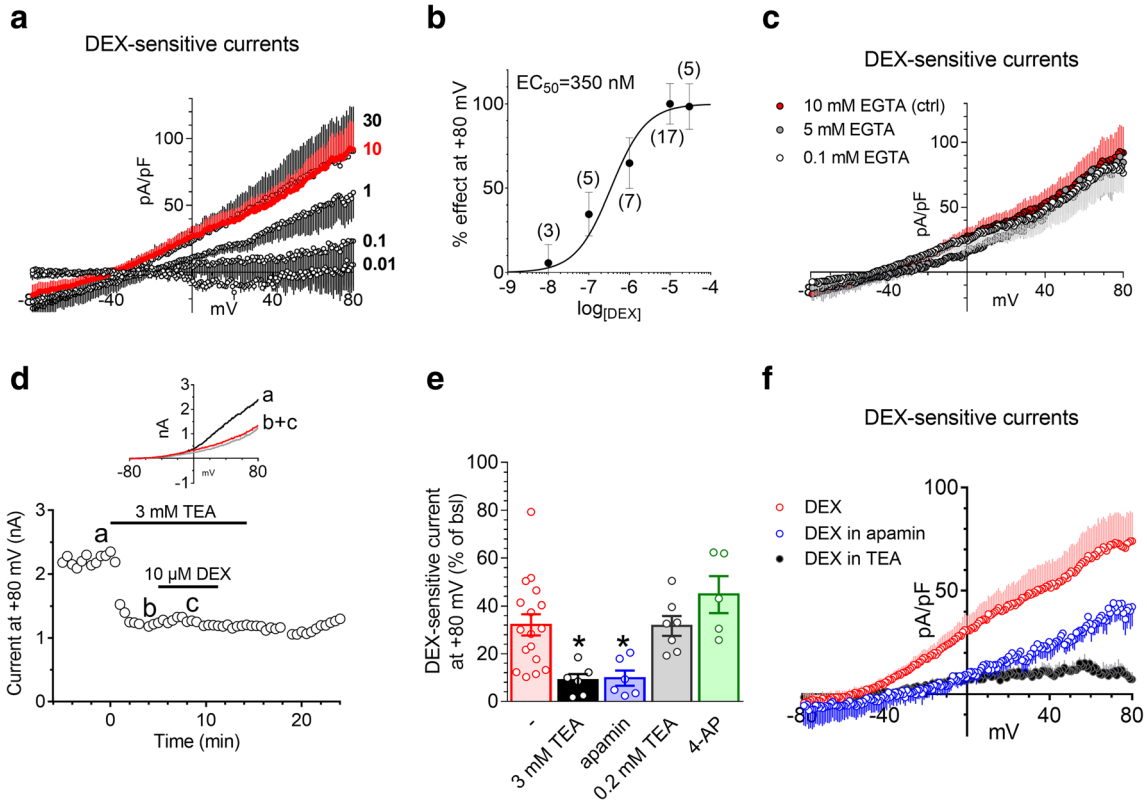

Fig. 2 The effect of DEX on outward K^+ currents is concentration-dependent and prevented by the K^+ channel blocker tetraethylammonium and by the selective small-conductance Ca^{2+}-dependent K^+ blocker apamin. **a** Averaged (mean ± SE) DEX-sensitive currents measured in the presence of different concentrations of DEX (0.01–30 μM). **b** Concentration-response curve of DEX effect on ramp-evoked currents measured at + 80 mV. EC_{50} = 350 nM (confidence limits: 107.2–1.14 μM). Number of cells investigated is written in parenthesis. **c** Averaged DEX (10 μM)-sensitive currents recorded by using different intracellular EGTA concentrations: control (ctrl) 10 mM EGTA (n = 15); 5 mM EGTA (n = 6), or 0.1 mM EGTA (n = 8). **d** Time course of ramp-evoked currents at + 80 mV recorded in a representative cell before, during, or after the application of 3 mM tetraethylammonium (TEA) alone or in combination with 10 μM DEX. Inset: original patch-clamp current traces recorded in the same cell at representative time points. **e** Pooled data of DEX-sensitive current recorded at + 80 mV in the absence (n = 15) or presence of different K^+ channel blockers: 3 or 0.2 mM TEA (n = 6 and n = 7, respectively); 100 nM apamin (n = 6) or 0.5 mM 4-aminopyridine (4-AP; n = 5). *p < 0.05, one-way ANOVA, Bonferroni post-test. **f** Averaged (mean ± SE) DEX-sensitive currents measured in the presence of different K^+ channel blockers

Discussion

In the present work, we show that acute DEX enhances outward K^+ currents in isolated hippocampal neurons and decreases synaptic transmission and pyramidal cell excitability in acute hippocampal slices. These effects are consistent with the ability of DEX to promote neuroprotection in hippocampal slices exposed to excitotoxicity or oxygen and glucose deprivation (OGD), as well as in multiple rodent models of cerebral ischemia [26, 27]. These findings complicate the pharmacodynamic profile of the drug, emphasizing its ability to interact with ion channels. These pleiotypic effects on neuronal conductances are in keeping with the structural similarity of DEX with riluzole, another pleiotypic ion channel modulator [9, 28], as well as toxins able to target multiple ion channels [24]. The present study, therefore, by adding an additional molecular target of DEX, emphasizes the complex pharmacodynamics underpinning the neuroprotective properties of these compounds. Originally, DEX-mediated neuroprotection was ascribed to its ability to function as an F1Fo ATP synthase activator leading to improved bioenergetics and inhibition of mitochondrial transition pore opening [2, 22]. Indeed, the compound increases neuronal ATP content and prevents mitochondrial swelling and permeability transition [6, 27, 29]. Accordingly, we previously ascribed the ability of DEX to completely prevent irreversible synaptic failure and anoxic depolarization in hippocampal slices exposed to OGD to its bioenergetic boosting effects [27]. However, we now reason that the compound's ability to increase outward K^+ currents shown in the present study may contribute to its neuroprotective effects by counteracting neuronal depolarization upon excitotoxic/ischemic insults. Indeed, the increase in outward K^+ conductance prompted by DEX can substantially hinder Ca^{2+} channel opening and ensuing glutamate release. This is well in keeping with previous findings showing the ability of DEX to reduce Ca^{2+} transients in cultured neurons [27], and with present data showing the ability of DEX to reduce fEPSP in CA1 dendrites upon Schaffer fiber stimulation.

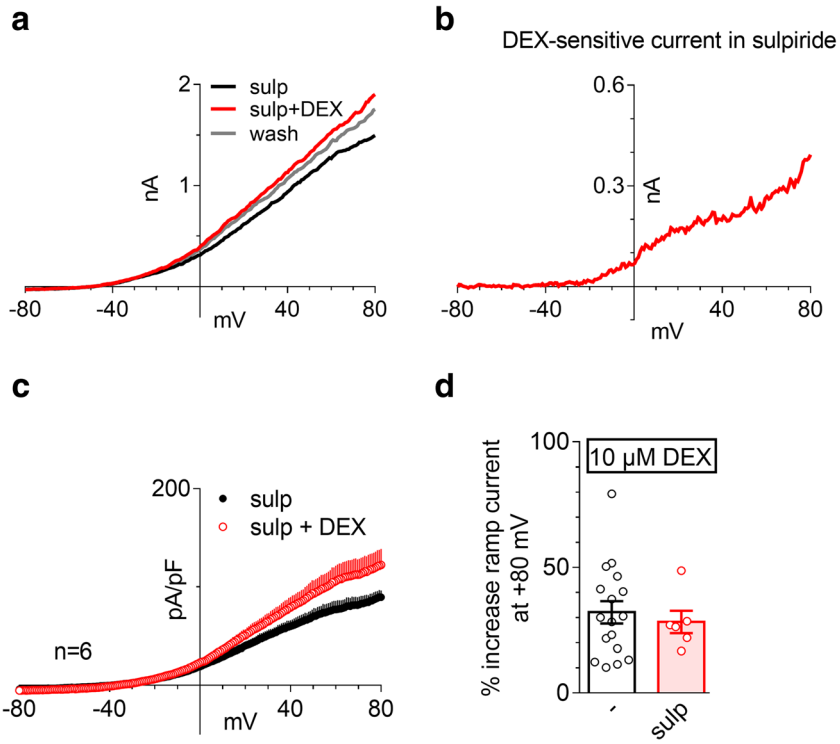

Fig. 3 The effect of DEX on outward K^+ currents is not prevented by the dopamine receptor antagonist sulpiride. **a** Original ramp current traces recorded in the continuous presence of sulpiride (1 μM) before (sulp), during (sulp + DEX), or after (wash) the application 10 μM DEX in a representative cell. **b** DEX-sensitive current, obtained by subtraction of the trace recorded in sulpiride from the ramp recorded in sulpiride + DEX, in the same cell. **c** Averaged (mean ± SE) ramp-evoked currents measured before or during DEX application in the presence of sulpiride in 6 cells tested. $^{**}p < 0.01$ paired Student's *t* test. d Pooled data of ramp-evoked currents at + 80 mV recorded in the absence ($n = 15$) or presence ($n = 6$) of sulpiride

Additionally, outward K^+ current increase shifts membrane potential away from AP threshold, thereby reducing the number of firing cells in the *stratum pyramidale*, and increasing their latency to achieve AP initiation, in principle two electrophysiological events further contributing to neuroprotection. Of note, DEX did not affect afferent fiber volley amplitude, thus indicating that the inhibitory effect of the compound does not depend on axonal conduction but rather on pre- and/or postsynaptic phenomena.

We show here that both TEA and apamin inhibit significant fractions of the outward ramp currents augmented by DEX indicating an involvement of Kv and SK channels, respectively. Notably, present data showing that the D2/D3 receptor antagonist sulpiride is unable to prevent DEX-dependent outward K^+ current increase indicate that the ion channel-modulating activity of DEX is independent of dopamine receptor activation, in keeping with its low D2/D3 receptor affinity [18].

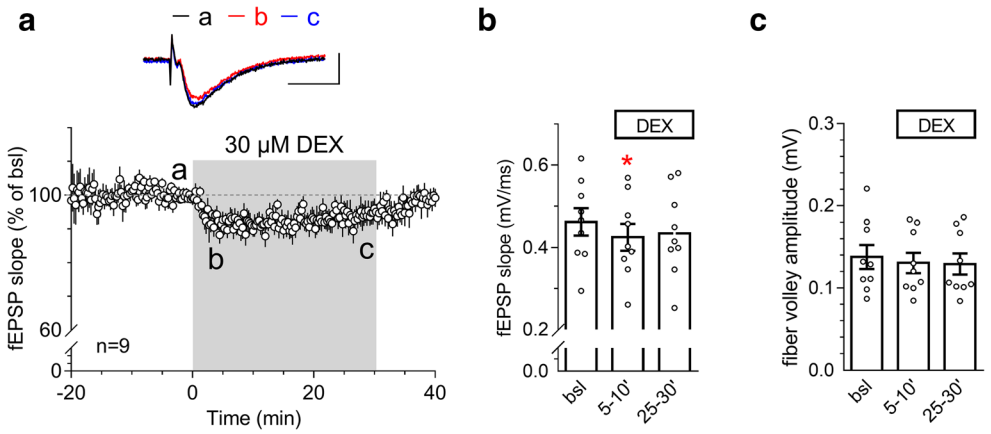

Fig. 4 DEX decreases fEPSP slope in the dendritic layer of CA1 hippocampal slices. **a** Time course of averaged (mean ± SE) fEPSP slope, normalized to respective baseline values (% of bsl), measured before, during, or after a 30 min application of DEX (30 μM) in CA1 rat hippocampal slices. Upper panel: original fEPSP traces recorded in a typical slice at representative time points: before DEX (**a**; black line trace), at 5 min DEX (**b**; red trace), or at 25 min DEX (**c**; blue trace). Scale bars: 0.5 mV; 10 ms. **b** Pooled data of fEPSP slope measured during bsl (last 5 min before DEX), at 5–10 min DEX, or at 25–30 min DEX. $^{*}p < 0.05$ vs bsl, paired Student's *t* test $n = 9$. **c** Pooled data of afferent fiber volley amplitude measured during bsl (last 5 min before DEX), at 5–10 min DEX or at 25–30 min DEX. No significant difference was found between groups, paired Student's *t* test $n = 9$

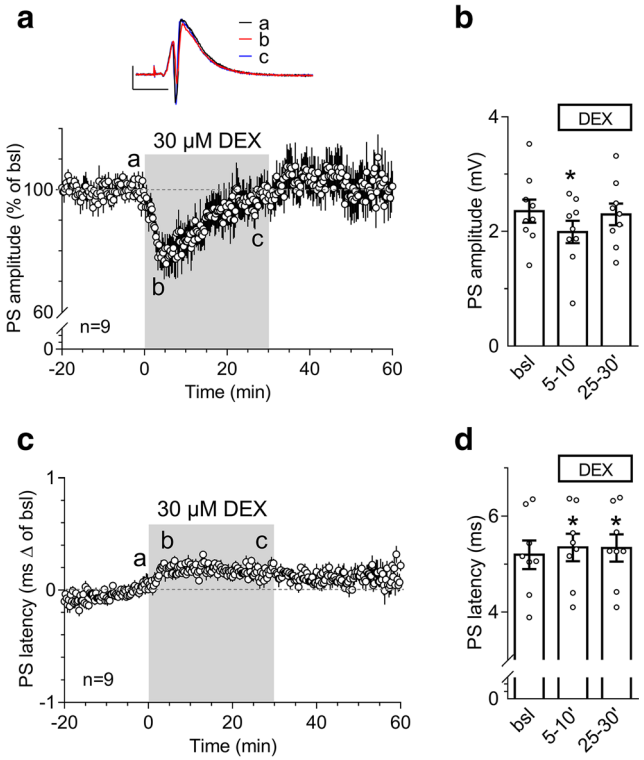

Fig. 5 DEX decreases PS amplitude and increases PS latency in the somatic layer of CA1 hippocampal slices. **a,c** Time courses of averaged (mean ± SE) PS amplitude (**a**) or latency (**c**), expressed as % of baseline (bsl) and measured before, during, or after a 30 min application of DEX (30 μM) in CA1 rat hippocampal slices. Upper panel in (**a**): original PS traces recorded in a typical slice at representative time-points: before DEX (**a**; black trace), at 5 min DEX (**b**; red trace), or at 25 min DEX (**c**; blue trace). Scale bars: 1 mV; 10 ms. **b,d** Pooled data of PS amplitude (**b**) or latency (**d**) measured during bsl (last 5 min before DEX), at 5–10 min DEX, or at 25–30 min DEX. *$p < 0.05$ vs bsl, paired Student's t test, $n = 9$

As we recently reported, DEX inhibits I_A in hippocampal neurons, thereby facilitating LTP induction in aged hippocampal neurons and preventing scopolamine-induced cognitive impairment [13]. Of note, when studied on I_A, DEX was pre-incubated in hippocampal slices for 30 min, an experimental protocol that precluded the possibility to detect a drug's impact on basal fEPSP. Furthermore, transient I_A conductance in isolated hippocampal neurons was evoked by short depolarizing voltage steps without overall ramp current induction. Finally, in that work [12], we did not observe any effect of DEX on steady-state K^+ currents evoked by the voltage step, possibly because the 100 ms step did not allow full development of sustained, delayed rectifier, I_K currents.

Even though the impact of DEX on I_A is in keeping with its pro-cognitive effects, it is unlikely that it also participates to define the neuroprotective potential of DEX during brain insults. Indeed, I_A current undergoes robust, voltage-dependent inactivation at potentials above -40 mV that are typical of injured neurons. Regardless, the ability of DEX to inhibit transient I_A2 and increase sustained K^+ currents indicates that the compound has a wide impact on K^+ conductances and can both promote and counteract synaptic transmission, depending upon the physiological/pathological condition of the brain tissue or the ion channel repertoire of neurons involved. As for the ability of DEX to selectively inhibit Nav1.8 channels [30], we rule out that this effect can contribute to DEX-dependent neuroprotection because Nav1.8 channel expression is absent in the rodent hippocampus [30] and mostly confined to the peripheral nervous system. Indeed, we previously demonstrated that DEX is devoid of effects on hippocampal Na^+ currents [30].

Of note, we report here that the inhibitory effect of DEX on fEPSP and PS amplitude faded before drug removal. Conversely, the increase of PS latency, which indicates the delay between fEPSP depolarization and action potential initiation in the cell soma, persisted throughout the application. Although at present we do not have an explanation for the molecular events underpinning these transient effects, we reason that the integrated nature of the hippocampal circuitry in the slices, as well as the lack of voltage clamping in this experimental setting, allow electrophysiological feedback responses capable of compensating some of the functional effects originating from increased outward K^+ currents.

In conclusion, we show here that DEX inhibits hippocampal electrical activity and increases TEA-sensitive K^+ conductances and SK-operated currents in hippocampal neurons.

Author's contributions EC and AC made substantial contributions to the conception or design of the work; EC, DB, GR, FC, and MV performed the experiments and analyzed data; EC, AMP, and AC worked on interpretation of data. EC drafted the work; AC and AMP revised it critically; AC approved the version to be published.

Funding The present work was supported by the University of Florence (Fondi Ateneo), by grants from Italian Foundation for Multiple Sclerosis (FISM) (2019/R-Single/036 (AMP and EC) and 2014/R/6 (AC)); by Fondazione Umberto Veronesi (EC), by PRIN 2017 (AC), Regione Toscana Progetto Salute 2018 (AC), AIRC, and Fondazione CR Firenze under IG 2017 - ID. 2045 (AC).

Data availability The datasets generated and analyzed during the current study are available from the corresponding author on reasonable request.

Declarations

The present research does not involve human participants. All animal procedures were conducted according to the Italian Guidelines for Animal Care, DL 26/2014, and authorized by the Italian Ministry of Health, Aut. N. 788/2016-PR.

Conflict of Interest The authors declare that they have no conflict of interest.

Consent to Participate Not applicable.

Consent for Publication Not applicable.

References

1. Alavian KN, Dworetzky SI, Bonanni L, Zhang P, Sacchetti S, Li HM, Signore AP, Smith PJS et al (2015) The mitochondrial complex V-associated large-conductance inner membrane current is regulated by cyclosporine and dexpramipexole. Mol Pharmacol 87:1–8
2. Alavian KN, Dworetzky SI, Bonanni L, Zhang P, Sacchetti S, Mariggio MA, Onofrj M, Thomas A et al (2012) Effects of dexpramipexole on brain mitochondrial conductances and cellular bioenergetic efficiency. Brain Res 1446:1–11
3. Anderson WW, Collingridge GL (2001) The LTP Program: a data acquisition program for on-line analysis of long-term potentiation and other synaptic events. J Neurosci Methods 108:71–83
4. Baj G, Patrizio A, Montalbano A, Sciancalepore M, Tongiorgi E (2014) Developmental and maintenance defects in Rett syndrome neurons identified by a new mouse staging system in vitro. Front Cell Neurosci:8
5. Barry PH (1994) JPCALC, a software package for calculating liquid-junction potential corrections in patch-clamp, intracellular, epithelial and bilayer measurements and for correcting junction potential measurements. J Neurosci Methods 51:107–116
6. Cassarino DS, Fall CP, Smith TS, Bennett JP (1998) Pramipexole reduces reactive oxygen species production in vivo and in vitro and inhibits the mitochondrial permeability transition produced by the Parkinsonian neurotoxin methylpyridinium ion. J Neurochem 71: 295–301
7. Cheah BC, Kiernan MC (2010) Dexpramipexole, the R(+) enantiomer of pramipexole, for the potential treatment of amyotrophic lateral sclerosis. Idrugs 13:911–920
8. Chiarugi A (2002) Characterization of the molecular events following impairment of NF-kappa B-driven transcription in neurons. Mol Brain Res 109:179–188
9. Cifra A, Mazzone GL, Nistri A (2013) Riluzole: what it does to spinal and brainstem neurons and how it does it. Neuroscientist 19: 137–144
10. Colotta V, Lenzi O, Catarzi D, Varano F, Squarcialupi L, Costagli C, Galli A, Ghelardini C et al (2012) 3-Hydroxy-1H-quinazoline-2, 4-dione derivatives as new antagonists at ionotropic glutamate receptors: molecular modeling and pharmacological studies. Eur J Med Chem 54:470–482
11. Coppi E, Cellai L, Maraula G, Dettori I, Melani A, Pugliese AM, Pedata F (2015) Role of adenosine in oligodendrocyte precursor maturation. Front Cell Neurosci 9
12. Coppi E, Cherchi F, Fusco I, Failli P, Vona A, Dettori I, Gaviano L, Lucarini E et al (2019) Adenosine A(3) receptor activation inhibits pronociceptive N-type Ca2+ currents and cell excitability in dorsal root ganglion neurons. Pain 160:1103–1118
13. Coppi E, Lana D, Cherchi F, Fusco I, Buonvicino D, Urru M, Ranieri G, Muzzi M et al (2018) Dexpramipexole enhances hippocampal synaptic plasticity and memory in the rat. Neuropharmacology 143:306–316
14. Coppi E, Pedata F, Gibb AJ (2012) P2Y(1) receptor modulation of Ca2 + -activated K+ currents in medium-sized neurons from neonatal rat striatal slices. J Neurophysiol 107:1009–1021
15. Cudkowicz M, Bozik ME, Ingersoll EW, Miller R, Mitsumoto H, Shefner J, Moore DH, Schoenfeld D et al (2011) The effects of dexpramipexole (KNS-760704) in individuals with amyotrophic lateral sclerosis. Nat Med 17:1652–U1169
16. Cudkowicz M, Van den Berg L, Shefner J, Mitsumoto H, Mora J, Ludolph A, Hardiman O, Ingersoll E et al (2013) Efficacy of Dexpramipexole in amyotrophic lateral sclerosis: data from the phase III EMPOWER trial. Neurology 80
17. Cudkowicz ME, van den Berg LH, Shefner JM, Mitsumoto H, Mora JS, Ludolph A, Hardiman O, Bozik ME et al (2013) Dexpramipexole versus placebo for patients with amyotrophic lateral sclerosis (EMPOWER): a randomised, double-blind, phase 3 trial. Lancet Neurol 12:1059–1067
18. Danzeisen R, Schwalenstoecker B, Gillardon F, Buerger E, Krzykalla V, Klinder K, Schild L, Hengerer B et al (2006) Targeted antioxidative and neuroprotective properties of the dopamine agonist pramipexole and its nondopaminergic enantiomer SND919CL2x (+)2-amino-4,5,6,7-tetrahydro-6-L-propylamino-benzathiazole dihydrochloride. J Pharmacol Exp Ther 316:189–199
19. Dworetzky SI, Hebrank GT, Archibald DG, Reynolds IJ, Farwell W, Bozik ME (2017) The targeted eosinophil-lowering effects of dexpramipexole in clinical studies. Blood Cells Mol Dis 63:62–65
20. Frey U, Schroeder H, Matthies H (1990) Dopaminergic antagonists prevent long-term maintenance of posttetanic LTP in the CA1 region of rat hippocampal slices. Brain Res 522:69–75
21. Fusco I, Ugolini F, Lana D, Coppi E, Dettori I, Gaviano L, Nosi D, Cherchi F et al (2018) The selective antagonism of adenosine A(2B) receptors reduces the synaptic failure and neuronal death induced by oxygen and glucose deprivation in rat CA1 hippocampus in vitro. Front Pharmacol 9
22. Jonas EA, Porter GA, Beutner G, Mnatsakanyan N, Alavian KN (2015) Cell death disguised: the mitochondrial permeability transition pore as the c-subunit of the F1FO ATP synthase. Pharmacol Res 99:382–392
23. Lee SI, Hoeijmakers JGJ, Faber CG, Merkies ISJ, Lauria G, Waxman SG (2020) The small fiber neuropathy NaV1.7 I228M mutation: impaired neurite integrity via bioenergetic and mitotoxic mechanisms, and protection by dexpramipexole. J Neurophysiol 123:645–657
24. Li-Smerin Y, Swartz KJ (1998) Gating modifier toxins reveal a conserved structural motif in voltage-gated Ca2+ and K+ channels. Proc Natl Acad Sci U S A 95:8585–8589
25. Licznerski P, Park HA, Rolyan H, Chen RM, Mnatsakanyan N, Miranda P, Graham M, Wu J et al (2020) ATP synthase c-subunit leak causes aberrant cellular metabolism in fragile X syndrome. Cell 182:1170-+
26. Muzzi M, Buonvicino D, Urru M, Tofani L, Chiarugi A (2018) Repurposing of dexpramipexole to treatment of neonatal hypoxic/ischemic encephalopathy. Neurosci Lett 687:234–240
27. Muzzi M, Gerace E, Buonvicino D, Coppi E, Resta F, Formentini L, Zecchi R, Tigli L et al (2018) Dexpramipexole improves bioenergetics and outcome in experimental stroke. Br J Pharmacol 175: 272–283
28. Samano C, Nistri A (2019) Mechanism of neuroprotection against experimental spinal cord injury by riluzole or methylprednisolone. Neurochem Res 44:200–213
29. Sayeed I, Parvez S, Winkler-Stuck K, Seitz G, Trieu I, Wallesch CW, Schonfeld P, Siemen D (2006) Patch clamp reveals powerful blockade of the mitochondrial permeability transition pore by the D2-receptor agonist pramipexole. FASEB J 20:556-+
30. Urru M, Muzzi M, Coppi E, Ranieri G, Buonvicino D, Camaioni E, Coppini R, Pugliese AM et al (2020) Dexpramipexole blocks Na(v)1.8 sodium channels and provides analgesia in multiple nociceptive and neuropathic pain models. Pain 161:831–841